

RSC Advances



This is an *Accepted Manuscript*, which has been through the Royal Society of Chemistry peer review process and has been accepted for publication.

Accepted Manuscripts are published online shortly after acceptance, before technical editing, formatting and proof reading. Using this free service, authors can make their results available to the community, in citable form, before we publish the edited article. This *Accepted Manuscript* will be replaced by the edited, formatted and paginated article as soon as this is available.

You can find more information about *Accepted Manuscripts* in the [Information for Authors](#).

Please note that technical editing may introduce minor changes to the text and/or graphics, which may alter content. The journal's standard [Terms & Conditions](#) and the [Ethical guidelines](#) still apply. In no event shall the Royal Society of Chemistry be held responsible for any errors or omissions in this *Accepted Manuscript* or any consequences arising from the use of any information it contains.

Cite this: DOI: 10.1039/c0xx00000x

www.rsc.org/xxxxxx

PAPER

Vibrational spectroscopic investigation on interaction of sago starch capped silver nanoparticles with collagen: A comparative physicochemical study using FT-IR and FT-Raman techniques

Abhishek Mandal,^{a,b} Santhanam Sekar,^b N. Chandrasekaran,^a Amitava Mukherjee,^{*a} and Thotapalli P. Sastry^{*b}

Received (in XXX, XXX) Xth XXXXXXXXXX 20XX, Accepted Xth XXXXXXXXXX 20XX

DOI: 10.1039/b000000x

In order to study the effect of sago starch as capping agent; the silver nanoparticles were synthesized via chemical reduction method using different concentrations of sago starch (0.1-10 μM). These capped silver nanoparticles were added to collagen matrix and scaffolds in the form of sponges developed via lyophilization and analyzed them by using vibrational FTIR and FT-Raman spectroscopic techniques. These vibrational spectroscopic techniques show that the starch molecules are adsorbed on the surface of Ag colloids via their hydrophilic ($-\text{OH}$ groups) moiety with the hydrophobic part exposed to possible interaction with collagen. Moreover, it was found that the increase of the starch concentration avoided aggregation and lead to formation of silver nanoparticles with lower size. Furthermore, sago starch in the concentration range 0.1-10 μM served as matrix suitable for encapsulation and gradually releasing silver nanoparticles that imparted strong antibacterial property to the collagen scaffolds fabricated for biomedical applications.

1. Introduction

Vibrational spectroscopic techniques namely, Infrared and Raman are used to elucidate the changes in structure, chemical composition and morphology obtained by monitoring the changes in vibrations of the bonds that exist at molecular level.¹⁻³ Fourier-transform Infrared (FT-IR) spectroscopy is an analytical tool often used in detecting the structural changes occurring in complex biological samples.^{4,5} Although the presence of water molecules in the biological samples causes hindrance, it interferes with the FT-IR spectra. Moreover, the simple instrumentation in addition to rapid data collection and processing due to better signal to noise ratio has enabled it as technique of choice for the evaluation of tissue specimens.^{2,6} Similarly, Fourier-transform Raman (FT-Raman) spectroscopy is also a powerful technique, which is complementary to FT-IR, utilizes the inelastic scattering of monochromatic light attained via laser excitation is non-invasive in nature and thus finds use in the analysis of biological specimens such as cells and tissues that have medical

applications.⁷⁻¹² In spite of the fact that the FT-Raman spectra exhibit weaker signals compared to FT-IR, the relatively low interference encountered due to presence of water assists in the investigation of samples of biological origin.^{13,14}

Collagen, a well-known biopolymer and structural protein abundantly present in the mammals is essential for tissue formation and regeneration of various organs.¹⁵ The desirable features such as biodegradability, improved biocompatibility and reduced antigenicity have enabled their use as scaffolds for tissue engineering and regenerative medicines.^{16,17} The extraction of collagen from different sources is well established and thus collagen based products have been used widely in various medical and biological applications.^{18,19} Among them, collagen derived from fish scales possess denaturation temperature similar to Achilles tendon and have served as alternate source due to reported transmissible diseases in bovine-based collagen products.²⁰

Nanoparticles, in particular, silver due to optical, electrical and high thermal conductivities have been utilized in applications such as catalysis, electronics, and biosensors.^{21,22} Moreover, AgNPs as antimicrobial agent have found use in various biological and medical applications such as sustained drug delivery²³, surgical catheters²⁴ and in the development of dressing materials for treatment of infected wounds.^{25,26} However, the tendency of silver nanoparticles to aggregate in solution reduces

^aCentre for Nano-Biotechnology, School of Bio-Sciences and Technology, VIT University, Vellore 632014, India. Tel: +91-416-220 2620; E-mail: amitav@vit.ac.in

^bBio-Products Laboratory, Council of Scientific and Industrial Research (CSIR)-Central Leather Research Institute, Chennai, India. Fax: +91-44-24911589; Tel: +91-44-24420709; E-mail: sastriyp@hotmail.com

their stability, which decreases the bactericidal action and restricts their applications in biomedical fields.²⁷

The polymers of synthetic and natural origins are widely used as capping agents that assist in preventing the aggregation and also stabilize the nanoparticles.^{28,29} Sago starch has been considered as one of the most abundant and inexpensive polysaccharides based biopolymer, which exerts excellent properties viz. superior biodegradability and biocompatibility.³⁰⁻³² The conjunction of silver nanoparticles with biopolymers namely, sago starch and collagen provide a way in fabricating nano biomaterials of potential biomedical applications.

In our recent investigation, sago starch has been used as a matrix to deliver non agglomerated silver nanoparticles and incorporated in collagen scaffolds to make them more biocompatible and useful for biomedical applications.³³ However, no report on the interaction of sago starch capped silver nanoparticles with collagen has been documented in detail at the molecular level. Therefore, it is worthwhile to perform a comparative study on the interaction of the collagen scaffolds impregnated with AgNPs capped by different concentrations of sago starch using vibrational spectroscopic techniques viz. FTIR and FT-Raman, which can stimulate further investigations.

2. Materials and Methods

2.1 Materials

Crude fish scales were collected from nearby fish market. Sago starch (MW 20×10^6) was also purchased from nearby local retail market. Silver nitrate (AgNO_3) and sodium borohydride (NaBH_4) were purchased from Sigma-Aldrich, St. Louis, Mo, USA. All the chemicals and reagents used were of analytical grade and purchased from Sigma-Aldrich. MilliQ water (specific conductance $2 \mu\text{S cm}^{-1}$) was used throughout the work.

2.2. Methods

UV-vis measurements were made on a Jasco Spectrophotometer Model UV-VIS-V530. Circular dichroism experiment was performed on spectropolarimeter (JASCO J-715 model). Fourier-transform Infrared (FTIR) and Fourier-transform Raman (FT-Raman) spectroscopic analyses were carried out using Perkin-Elmer Spectrum 2000 instrument and Bruker: RFS27 (laser 100 mW), respectively. Scanning electron microscopic (SEM) analyses were carried out on Philips XL-30. The particle size analyses were confirmed using Malvern instruments, Model No. Zetasizer 3000 HS_A. Size and diffraction pattern of the silver nanoparticles were determined using a High resolution transmission (HRTEM) electron microscope (FEI, Technai T30 G2).

2.3. Extraction of fish scale collagen (C)

The isolation of collagen from scales of the marine fish, *Lates Calcarifer* was performed following the protocol reported earlier.¹⁹ In brief, the collected fish scales were subjected to washing with copious amounts of water to eliminate sand and other foreign bodies and subsequently exposed under sunlight. 500 g of these dried scales were soaked in 10% H_2SO_4 solution for 24 h and then thoroughly minced using a mincer. The resultant fine paste was subjected to centrifugation (12,000 rpm) at 4 °C for 20 mins. This supernatant was collected and its pH was adjusted to 7 by using saturated $\text{Ca}(\text{OH})_2$ solution. Further, centrifugation at 10,000 rpm for 15 mins was carried out to remove CaSO_4 salts. The supernatant had collagen solids (60%), which were stored at 4 °C.

2.4. Synthesis of silver nanoparticles (AgNPs)

The experiment was performed in a dark room at 4 °C. To 1 mL of 0.01 M AgNO_3 solution, 5 mL of 0.02 M NaBH_4 solution was added dropwise with continuous stirring for 20 min. The appearance of pale yellow color indicates the formation of silver nanoparticles in the solution.

2.5. Synthesis of sago starch capped silver nanoparticles (SGAgNPs)

Using a domestic mixer, sago was sieved and powdered. Different weights (0.1, 0.5, 1, 5 and 10 g) of sago starch were dissolved in 50 mL milliQ water by heating at 50 ± 5 °C to obtain the concentrations of 0.1, 0.5, 1, 5 and 10 μM , respectively. The contents were added to 1 mL of 0.01 M AgNO_3 solution. Subsequently, 5 mL of 0.02 M NaBH_4 solution was added dropwise with continuous stirring for 20 mins to ensure the completion of the reaction. The above experiment was conducted in a dark cold room at 4 °C.

2.6. Preparation of collagen scaffolds impregnated with sago starch capped AgNPs (C-SG-AgNPs)

To the beaker containing 10 mL of the fish scale collagen solution, added 10 mL of silver nanoparticles solution with continuous stirring by the magnetic stirrer. The process of stirring was continued for 15 min. The contents were transferred in petriplates and subjected to lyophilization to obtain scaffolds in the form of sponges. The details regarding the above preparations, we have described in our recent publication.³³

3. Results and Discussion

UV-vis spectra (Fig. 1) show characteristic peak of the silver surface plasmon resonance (SPR) at around 400 nm, which suggests the generation of AgNPs.^{34,35} This characteristic peak

was further red-shifted to 401, 403, 406, and 415 nm for silver nanoparticles capped by 0.1, 0.5, 1 and 5 μM concentrations of sago starch, respectively. However, at the highest concentration of sago starch (10 μM) used in this study, the SPR peak of AgNPs was noticed at 404 nm and this decrease in shift indicates the aggregation of nanoparticles.

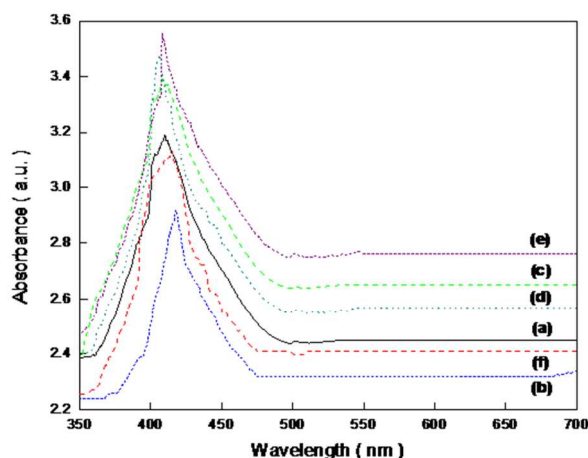


Fig. 1 UV-Vis spectra of silver nanoparticles uncapped (a) and capped by (b) 0.1 μM , (c) 0.5 μM , (d) 1 μM , (e) 5 μM and (f) 10 μM sago starch, respectively.

Particle size analyzer (PSA) was used to determine the particle size of the sago starch capped AgNPs. The AgNPs capped by 0.1 μM sago starch were obtained in the range of 45-80 nm compared to 50-100 nm for the uncapped AgNPs. Moreover, the particle sizes for AgNPs capped by 0.5, 1, 5 and 10 μM sago starch, as shown in Fig. 2 were found to be in the range of 35-75 nm, 30-60 nm, 15-40 nm and 40-85 nm, respectively. The reduction in the size of AgNPs was observed up to 5 μM concentration of sago starch. Further increase in concentration of capping agent, sago starch (10 μM) results in their aggregation and thus an increase in particle size was noted.

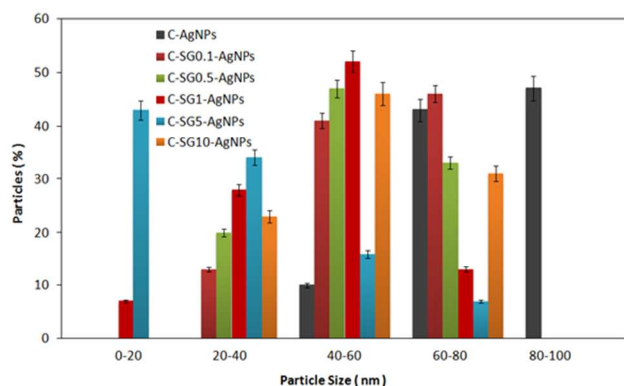


Fig. 2 Particle size analysis of synthesized silver nanoparticles: a) uncapped, b) 0.1 μM , c) 0.5 μM , d) 1 μM , e) 5 μM and f) 10 μM sago starch, respectively.

Collagen extracted from the fish scales was confirmed by circular dichroism (CD) spectroscopy. The CD spectrum depicted in Fig. 3 has two bands at 201 and 229 nm due to π - π^* amide and positive n- π^* transitions, respectively. The intensity of these two characteristic bands used to measure the triple helical content and thereby confirms the presence of collagen molecules.³⁶

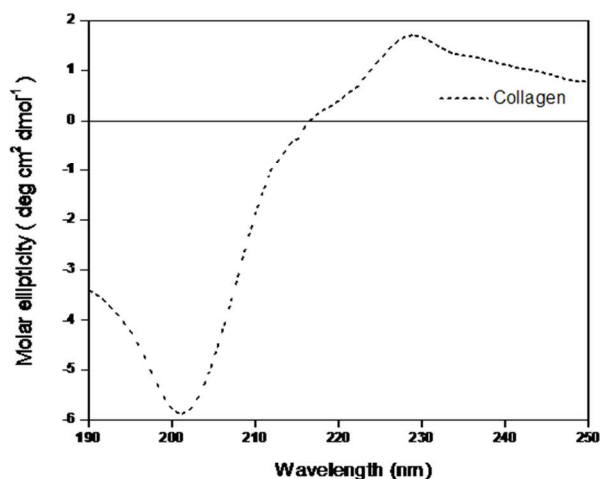


Fig. 3 Circular dichroism (CD) spectrum of collagen isolated from *Lates Calcarifer* fish scales.

FTIR spectroscopy was used to classify and characterize the collagen based scaffolds to understand the interaction between the sago starch encapsulated AgNPs with template type I collagen (See Figs. 4 and 5). The FT-IR spectroscopic data for collagen based scaffolds containing uncapped silver nanoparticles (C-AgNPs) and different concentrations of sago starch encapsulated AgNPs at 20°C are depicted in Table 1.

<Insert Table 1 here>

The spectrum of collagen scaffold alone (Fig. 4(b)) in addition to the O-H stretching band observed at 3200 cm^{-1} exhibit characteristic amide I, II and III bands located at the finger print region (800-1500 cm^{-1}) respectively. Similarly, the characteristic bands of starch can be observed in four regions: (i) below 800 cm^{-1} , (ii) 800-1500 cm^{-1} (the finger print region), (iii) 2800-3000 cm^{-1} (C-H stretch region), and (iv) the region between 3000 and 3500 cm^{-1} (O-H stretch region), respectively.³⁷ In the present investigation, sago starch shows (see Fig. 4(a)) an absorption band between 3215-3536 cm^{-1} , which represents O-H stretch and a band at 2926 cm^{-1} due to the C-H stretching vibrations of the molecule. Also, other notable bands in the finger print region are the peak at 1230 cm^{-1} due to CH_2OH and 1142 cm^{-1} signifying coupling mode of C-C, C-O stretching vibrations, while the band at 1091 cm^{-1} denotes the C-O-H bending vibration. Moreover, a peak at 926 cm^{-1} is due to the vibrations of α -1,4-glycosidic linkage that occurs in the sago starch molecule.

The region below 800 cm^{-1} show bands at 659 and 461 cm^{-1} , which are denoted as the skeletal mode of pyranose ring respectively. Additionally, the spectrum of sago starch displayed the characteristic peaks associated with carbohydrates at 514 and 520 cm^{-1} , respectively. Moreover, peak at 2934 cm^{-1} was observed, which is attributed to the $-\text{CH}$ stretching and a broad band noticed in the region $3200\text{--}3500\text{ cm}^{-1}$ is associated to the stretching of hydroxyl groups ($-\text{OH}$) present in the sago starch, respectively.³¹

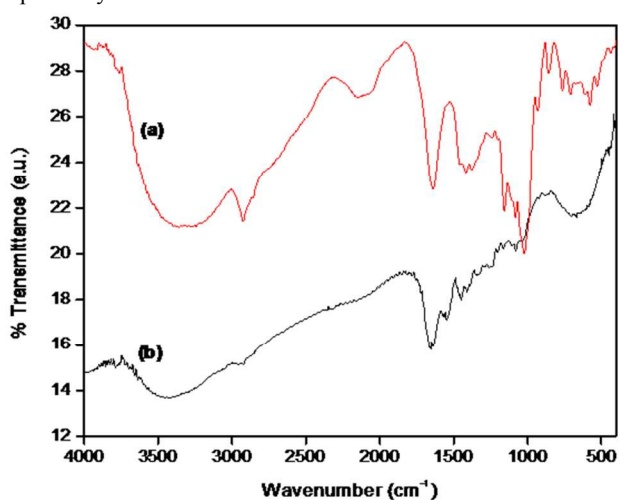


Fig. 4 FT-IR spectra of a) sago starch and b) collagen scaffold respectively.

The effect of different concentrations ($0.1\text{--}10\text{ }\mu\text{M}$) of sago starch on the encapsulation of AgNPs in collagen scaffolds were studied in the present investigation and are illustrated in Fig. 5.

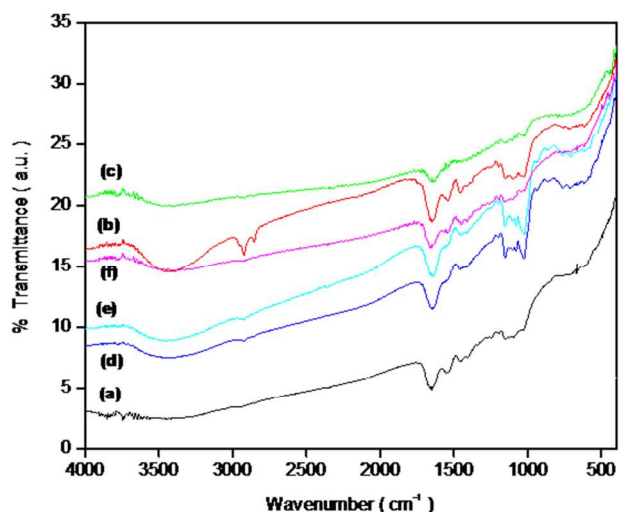


Fig. 5 FT-IR spectra of various collagen based scaffolds: a) C-AgNPs, b) C-SG0.1-AgNPs, c) C-SG0.5-AgNPs d) C-SG1-AgNPs e) C-SG5-AgNPs and f) C-SG10-AgNPs, respectively.

In collagen scaffolds containing uncapped AgNPs, it was found that the peak at 3240 cm^{-1} due to $-\text{OH}$ group contribution of the collagen moiety was shifted to 3261 cm^{-1} upon interaction with AgNPs. The extent of broadness of this band due to the contribution of hydroxyl groups (O-H) of starch diminishes and narrows down to 3261 cm^{-1} as a result of Van der Waals interaction with silver nanoparticles. This characteristic band was further shifted to higher regions $3289\text{--}3291\text{ cm}^{-1}$ in collagen scaffolds impregnated with sago starch encapsulated silver nanoparticles where the sago starch concentrations were varied from 0.1 to $10\text{ }\mu\text{M}$. This is based on the fact that sago starch also shows a broad band from 3100 to 3600 cm^{-1} attributed to the vibration of $-\text{OH}$ group present in the molecule. Thus, a shift in the band position was noted when the concentration of the starch was varied from 0.1 to $10\text{ }\mu\text{M}$, used in the capping of silver nanoparticles where the $-\text{OH}$ groups of the starch molecules interact with the partial positive charge that exists at the AgNPs surface. However, the peaks of starch at 1083 and 1022 cm^{-1} attributed to the anhydrous glucose ring (O-C stretching) appears to be broad in the presence of silver nanoparticles and a red-shift was noted with increase in starch concentration. This is most probably due to the coating of silver nanoparticles with starch. Similarly, the C-H stretching peak of starch at 2934 cm^{-1} gets diminished and disappeared with the increase in starch concentration, which again indicated the interaction of silver nanoparticles with that of starch. Moreover, the absence of band observed at 1384 cm^{-1} confirms that starch facilitates the complete reduction of Ag^+ to Ag^0 .³⁸ Also, the disappearance of peak at 2122 cm^{-1} indicates that the reduction of silver ions is coupled to the oxidation of hydroxyl groups, which signifies the oxidized nature of the starch. Based on the above observed shifts in bands and peaks associated to the hydroxyl groups, it can also be inferred that these groups present in the starch are involved in the synthesis of AgNPs and act as nanoscopic templates. In addition to this, other characteristic peaks of sago starch were observed in the finger print regions viz. 1075 and 950 cm^{-1} . The C-OH band at 1075 cm^{-1} is slightly red shifted in the case of AgNPs capped with increasing sago starch concentration from 0.1 to $10\text{ }\mu\text{M}$, which is most probably due to change in amorphous nature of the native starch to its semi-crystalline state in the presence of AgNPs.^{39,40} Moreover, the broad peak observed at 1646 cm^{-1} is due to the tightly held bound water present in the starch and the band at 2925 cm^{-1} indicates the C-H stretching vibration. The shift in the peaks is observed with the increase in starch concentration and this effect is most probably due to the encapsulation of sago starch on the silver nanoparticles. The characteristic bands of both collagen and starch, were observed in the above FTIR spectra of the scaffolds. However, the shifting of the bands in the fingerprint regions viz. from 950 to 1075 cm^{-1} and 1425 to 1420 cm^{-1} are observed. This is due to the interaction between $-\text{NH}_2$ groups of collagen and $-\text{OH}$ groups of starch.³³ In these scaffolds, the prominent amide I and II bands located at 1650 and 1538 cm^{-1} , respectively and the peaks observed in the

region, 1143-1301 cm^{-1} attributed to amide III (C–N stretching and N–H stretching), are due to presence of amines in glycine and proline residues of the collagen. These bands though shifted occur in all collagen scaffolds containing both uncapped and capped AgNPs, the shift results from the strong association of the amines in the collagen molecules with AgNPs through covalent/electrostatic bond formation.⁴¹ The transmittance ratio T_{1454}/T_{1234} usually used to study the helical nature of the proteins was close to 0.9 in all the scaffolds, which indicates that the triple helical structure of collagen remains intact and is not perturbed by sago starch.^{27,42} Furthermore, this also ascertains and verifies that the chemical interaction occurs between sago starch and collagen in the scaffolds.

FT-Raman spectroscopy was also used to characterize collagen-based scaffolds in order to assess the interaction between template type I collagen and AgNPs capped by different concentrations of sago starch. To classify, Raman spectra of collagen scaffolds containing uncapped AgNPs and different concentrations of capping agent, sago starch in the region 50-4000 cm^{-1} have been illustrated in Fig. 6.

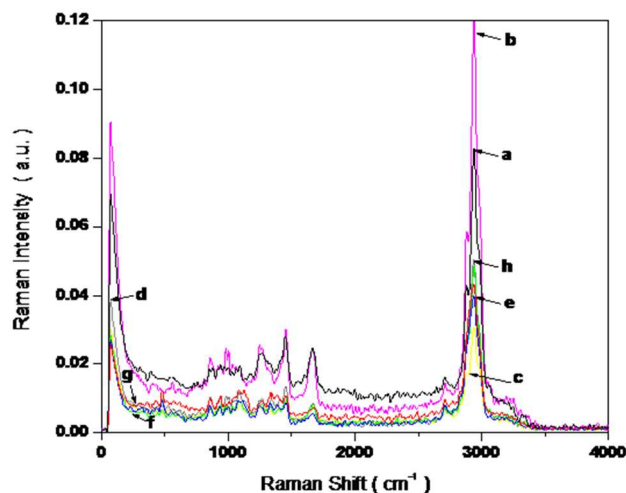


Fig. 6 FT-Raman spectra of various collagen based scaffolds: a) collagen alone b) C-AgNPs, c) C-SG0.1-AgNPs, d) C-SG0.5-AgNPs e) C-SG1-AgNPs f) C-SG5-AgNPs and g) C-SG10-AgNPs, respectively.

Collagen is a well-known structural protein in mammals and thus the spectrum of collagen scaffold alone depicts distinct bands of proteins in the region 300-3500 cm^{-1} . The peaks in the region 200-400 cm^{-1} are usually associated with the triple helicity of the collagen.⁴³ In the present investigation, the peaks observed at 304 and 391 cm^{-1} confirm the triple helical structure of collagen derived from the scales of *Lates Calcarifer*. Similarly, in all the collagen-based scaffolds, these peaks in the aforementioned region were present, which indicated that the triple helicity of collagen is intact. Additionally, strong band located at 1665 cm^{-1} assigned to amide I contributions is ascribed

mostly to the C=O stretching vibrations, and to some extent, C–N stretching, C α –C–N bending, along with the N–H in-plane bending of peptide groups.^{44,45} Moreover, a weak amide II band at 1510-1550 cm^{-1} due to N–H in-plane bending and C–N stretching vibrations of the peptides and amide III bands at the region, 1200-1300 cm^{-1} arising mainly from the vibrations of C–N stretching and N–H in plane bending modes of the peptide bond were observed. Also, the faint peaks noted in the 2400–2600 cm^{-1} region are due to S–H stretching vibrations of sulfhydryl groups present in the amino acids residues of collagen.⁴⁶

The strong peak at 2939 cm^{-1} (Fig. 6) is due to C–H stretching vibrations of the collagen. Similarly, this peak is also observed in the case of sago starch (data not shown here). Therefore, broadening of this peak in the case of collagen scaffolds impregnated with sago starch capped silver nanoparticles was observed and maximum in the case of C-SG10AgNPs. The information from the spectra profile of the amide I band has significant importance, as it provides a correlation between the frequencies of the amide I band and the extent of different residues present in protein backbone, which assists in deducing and deciphering its secondary structure.^{42,47-52} The amide I bands were located at 1665 and 1661 cm^{-1} for collagen scaffold alone and with uncapped AgNPs respectively. This band was also noticed around 1667-1673 cm^{-1} in the case of collagen scaffolds containing sago capped AgNPs. This observation indicates that all the collagen based scaffolds possess high α -helical content. Also, the intensity of the amide III band centered around 1252-1267 cm^{-1} due to vibrations from C α –C stretching and C=O in-plane bending modes,⁴³ which corroborate the α -helical structure of the collagen molecule noted in all the developed scaffolds.

<Insert Table 2 here>

The complex formation of AgNPs with the capping agent, sago starch results in i) splitting of bands in the 950-1200 cm^{-1} region and ii) red shifts noted for $\delta(\text{C–C–O})$ and $\delta(\text{C–O–C})$ bending modes that occur in the 500-600 cm^{-1} region with increase in starch concentration from 0.1 to 10 μM . These observed changes in the FT-Raman spectra suggest strong chemisorptions on the surface of capped AgNPs via coordination that occur when the lone pair of electrons from etheric oxygen atoms of starch molecule is donated to Ag^+ ($n \geq 1$) species that exist on its surface. Moreover, coordination of this type effect in decrease in the flexibility of the starch molecules and prefers a single favourable conformation, which was influenced by the large number of –OH groups of starch on the AgNPs surface.⁵³ Collagen scaffold impregnated with uncapped AgNPs shows bands at 859 and 879 cm^{-1} due to CH_2 rocking modes suggest the presence of different conformations. However, in the case of sago starch capped AgNPs, the existence of only band at 859 cm^{-1} ,

which is slightly red-shifted with increasing starch concentrations (see Table 2) indicates the preference of a single conformation on the Ag surface. Moreover, two groups of weaker bands are noted at 1126, 1083, 1036 and 970 cm^{-1} , respectively. The appearance of these newer bands is attributed to weakening of C–O bond that result in the decoupling of C–O and C–C vibrational modes, which effect the electron donation from oxygen (present in the hydroxyl groups of starch) to silver and thus, the chemisorptions occur in the preferred conformation.⁵⁴ Also, the collagen scaffold impregnated with starch capped AgNPs show a peak at 235 cm^{-1} , which is ascribed to the stretching vibrations of Ag–N and Ag–O bonds formation.⁵⁵ The appearance of this peak also signifies the chemical bond formation between silver and amino nitrogen and also with hydroxyl groups of the collagen and starch molecules, respectively. Thus, the sago starch is bound to the AgNPs surfaces by means of hydroxyl groups. Since, the vibrational frequencies of both Ag–N and Ag–O stretching modes are close to each other, it is noticed that the increase in sago starch concentrations result in peak broadening due to the involvement of both N and O atoms in bond formation.³⁷ The rate of aggregation of the absorbate, AgNPs depends on its adsorption rate by the adsorbent, sago starch in this case, as formation of larger aggregates are induced when the adsorption occurs via destruction of the original surface and dielectric bilayer that stabilizes the isolated colloidal AgNPs. Thus, the rate of aggregation of AgNPs capped by sago starch decreased with the increase in starch concentration initially upto 5 μM . However, the above rate of aggregation was highest in C-SG10AgNPs with higher particle size.

It is well known that higher concentrations of collagen results in the aggregation of the nanoparticles.^{41,56} Therefore, in the present investigation, the Ag colloids and collagen were mixed in the ratio 1:1 (v/v) to restrict the aggregation of the synthesized silver nanoparticles. With regard to the effect of sago starch as capping agent on the synthesis of silver nanoparticles and their interaction with collagen, it was evident from the scanning electron microscopic (SEM) images shown in Fig. 7 that at lower concentration of sago starch (0.1 μM), the adherence of silver nanoparticles on the collagen surface is limited. However, at highest sago starch concentration (10 μM) used in this study, the formation of large agglomerates were observed when AgNPs were added into the collagen solution. Thus, the optimum concentration of sago starch that prevents agglomeration and results in stable and monodispersed AgNPs was found to be 5 μM beyond which the aggregation occurs on the surface of collagen scaffolds. The energy dispersive X-ray spectroscopy (EDX) spectra displayed in Fig. 8 have signals of carbon and oxygen atoms apart from signals of the silver atoms present in the nanoparticles.

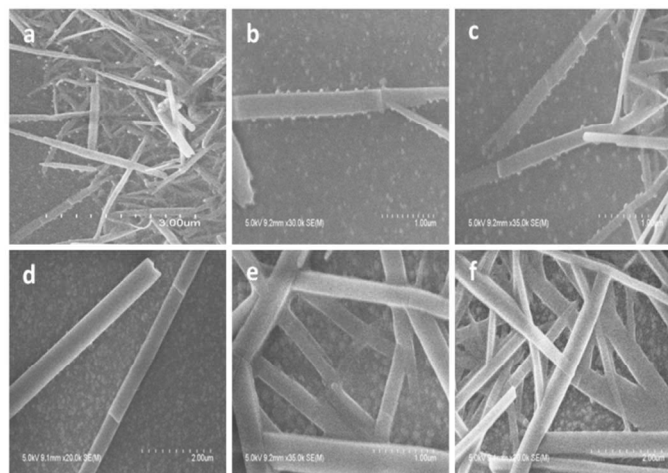


Fig. 7 SEM images of collagen based scaffolds: a) C-AgNPs; b) C-SG0.1-AgNPs; c) C-SG0.5-AgNPs; d) C-SG1-AgNPs; e) C-SG5-AgNPs and f) C-SG10-AgNPs respectively.

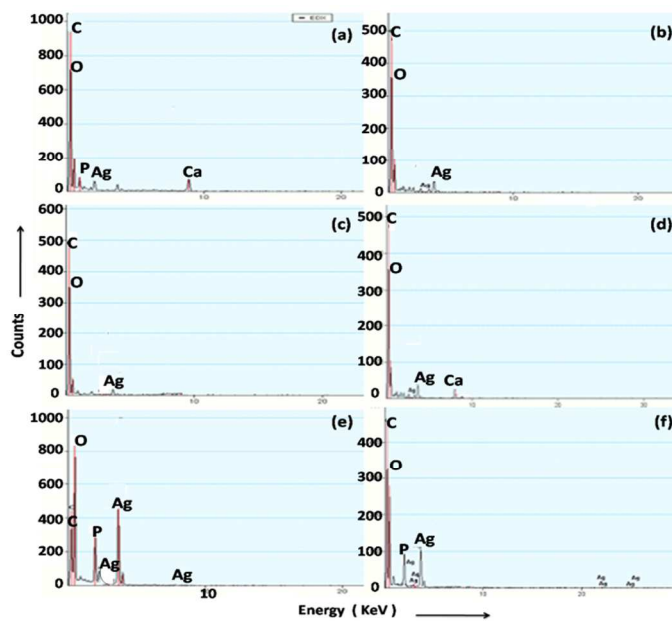


Fig. 8 EDAX spectra of scaffolds: a) C-AgNPs; b) C-SG0.1-AgNPs; c) C-SG0.5-AgNPs; d) C-SG1-AgNPs; e) C-SG5-AgNPs and f) C-SG10-AgNPs respectively.

HRTEM was used to examine the starch capped silver nanoparticles present in the collagen based scaffolds and selected area electron diffraction (SAED) was used to determine the effect sago starch has on the controlled size of AgNPs and on their crystal properties. The HRTEM images illustrated in Fig. 9 reveal the spherical morphology of the starch capped silver nanoparticles. The reduction of Ag^+ to Ag occurs inside the starch molecule and the hydroxyl groups present in the nanoscopic starch templates behave as passivation contacts for the

nanoparticle stabilization. The reduction of Ag^+ to Ag^0 occurs inside the starch molecule and the hydroxyl groups present in the nanoscopic starch templates act as passivation contacts for the nanoparticle stabilization. Therefore, starch serves both as reducing agent as well as performs the role of stabilizer.

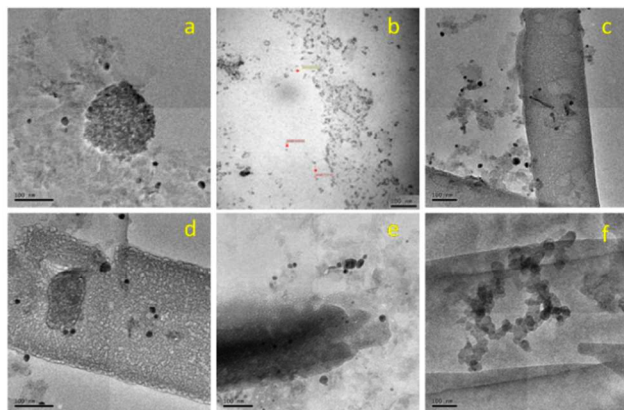


Fig. 9 HRTEM images of collagen based scaffolds: a) C-AgNPs; b) C-SG0.1-AgNPs; c) C-SG0.5-AgNPs; d) C-SG1-AgNPs; e) C-SG5-AgNPs and f) C-SG10-AgNPs respectively.

From the SAED pattern shown in Fig. 10, the silver nanoparticles appear to be twinned. It was found that the SAED data was in agreement with fcc structure of silver [57]. The SAED pattern with bright circular rings corresponding to (111), (200), (220) and (311) planes displayed the crystallinity of AgNPs. The growth of AgNPs occurred on (111) plane. The lattice spacing of the AgNPs was calculated using the following equation:

$$d = \lambda l / r$$

Where d is the lattice spacing, λ is the wavelength of the electrons, l is the camera focal length and r is the distance between the central spot and the diffracted spot or ring. The calculated $d_{(hkl)}$ values of the collagen based scaffolds containing both uncapped and different concentrations (0.1-10 μM) of sago starch capped silver nanoparticles were compared with the JCPDS File No. 04-0783 [58] and are provided in Table 3.

<Insert Table 3 here>

Increase in sago starch concentration leads to the formation of polycrystalline AgNPs. At the highest sago starch concentration (10 μM), the AgNPs are completely wrapped or present inside the starch molecule and so the SAED pattern of C-SG10-AgNPs (Fig. 10f) show a slightly diffuse band which indicates the partial crystalline nature of the starch capped AgNPs. The electron-donating effect of oxygen atoms from the large number of hydroxyl groups of the starch molecule exerts a

coordinative saturation of dangling bonds on the silver nanoparticle surface and enhances their stability when impregnated in the collagen scaffolds.²⁷ Moreover, this kind of controlled size synthesis of sago starch capped silver nanoparticles could be used as a catalyst for the synthesis of 2-aryl substituted benzimidazoles which have various biomedical applications.⁵⁹

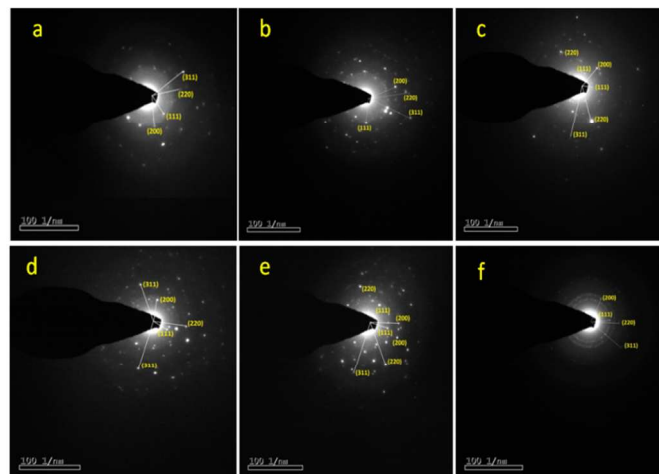


Fig. 10 SAED images of the collagen based scaffolds: a) C-AgNPs; b) C-SG0.1-AgNPs; c) C-SG0.5-AgNPs; d) C-SG1-AgNPs; e) C-SG5-AgNPs and f) C-SG10-AgNPs respectively.

4. Conclusions

The stable silver nanoparticles (AgNPs) capped by sago starch of different concentrations (0.1-10 μM) were successfully synthesized. These nanoparticles of different sizes were added to collagen and lyophilized to obtain sponges used as scaffolds. The FTIR and FT-Raman spectroscopic techniques show that the AgNPs are adsorbed on the surface of starch molecules via their hydrophilic moiety ($-\text{OH}$ groups) and possibly interacts with the hydrophobic part of collagen. The FT-Raman spectra suggest strong chemisorptions on the surface of starch capped AgNPs via coordination that occur when the lone pair of electrons from etheric oxygen atoms of starch molecule is donated to Ag^+ ($n \geq 1$) species that exist on its surface. Moreover, coordination of this kind of effect in decreasing the flexibility of the starch molecules and prefers a single favorable conformation. The FTIR and FT-Raman spectroscopies also reveal that increase of the starch concentrations avoids aggregation and lead to formation of silver nanoparticles with lower size upto sago starch concentration of 5 μM , which was optimum. However, higher concentration of sago starch (10 μM) results in the nanoparticle aggregation with higher size. Thus, the green approach involved in the synthesis show sago starch of extremely low and high concentrations (0.1-10 μM) acting as template and also as matrix for encapsulation and

gradual release of silver nanoparticles, which can provide strong antibacterial property to the collagen scaffolds prepared for biological and biomedical applications.

Acknowledgements

The authors are grateful to Prof. Dr. Asit Baran Mandal, Director, CSIR-Central Leather Research Institute, Chennai, India, for granting permission to carry out the experiments in the institute. The authors are also grateful to Prof. S. Balakumar, Director of National Centre for Nanosciences and Nanotechnology, University of Madras for stimulating discussion regarding SAED analysis and providing HRTEM facility.

References

- 1 A. Falamas, S. Cinta-Pinzaru, C. Dehelean, C. H. Krafft and J. Popp, *Romanian J. Biophys.*, 2010, **20**, 1–11.
- 2 C. Krafft and V. Sergio, *Spectroscopy*, 2006, **20**, 195–218.
- 3 P. T. T. Wong, *Proc. AIP*, 1993, **309**, 1431–1434.
- 4 U. C. Kemas, E. I. Nep, A. A. Agbowuro and N. A. Ocheke, *World Journal of Pharmaceutical Research*, 2012, **1**, 1234–1249.
- 5 G. Deleris and C. Petibois, *Vib. Spectrosc.*, 2003, **32**, 129–136.
- 6 M. Diem, S. S. M. Boydston-White and L. Chiriboga, *Appl. Spectrosc.*, 1999, **53**, 148–161.
- 7 A. Power, J. Cassidy and T. Betts, *Analyst*, 2011, **136**, 2794–2801.
- 8 X. M. Qian, and S. M. Nie, *Chem. Soc. Rev.*, 2008, **37**, 912–920.
- 9 J. Kneipp, H. Kneipp, A. Rajadurai, R. W. Redmond and K. Kneipp, *J. Raman Spectrosc.*, 2009, **40**, 1–5.
- 10 W. Lo, J. Lai, S. E. Feinberg, K. Izumi, S. Kao, C. Chang, A. Lin and H. K. Chiang, *J. Raman Spectrosc.*, 2011, **42**, 174–178.
- 11 P. Wu, Y. Gao, Y. Lu, H. Zhang and C. Cai, *Analyst*, 2013, **138**, 6501–6510.
- 12 C. Krafft, S.B. Sobottka, G. Schackert and R. Salzer, *Analyst*, 2005, **130**, 1070–1077.
- 13 F. Bonnier, A. Mehmood, P. Knief, A. D. Meade, W. Hornebeck, H. Lambkin, K. Flynn, V. McDonagh, C. Healy, T. C. Lee, F. M. Lyng and H. J. Byrne, *J. Raman Spectrosc.*, 2011, **42**, 888–896.
- 14 H. Cheng, S. Huan and R. Yu, *Analyst*, 2012, **137**, 3601–3608.
- 15 G. A. Di Lullo, S. M. Sweeney, J. Korkko, L. Ala-Kokko and J. D. San Antonio, *J. Biol. Chem.*, 2002, **277**, 4223–4231.
- 16 A. Mandal, S. Panigrahi and C. Zhang, *Biol. Eng. ASABE*, 2010, **2**, 63–88.
- 17 A. K. Lynn, I. V. Yannas and W. Bonfield, *J. Biomed. Mater. Res. B*, 2004, **71**, 343–354.
- 18 A. Mandal, S. Sekar, M. Kanagavel, N. Chandrasekaran, A. Mukherjee and T. P. Sastry, *Biochim. Biophys. Acta*, 2013, **1830**, 4628–4633.
- 19 S. Sankar, S. Sekar, R. Mohan, R. Sunita, J. Sundaraseelan, and T. P. Sastry, *Int. J. Biol. Macromol.*, 2008, **42**, 6–9.
- 20 F. Pati, B. Adhikari, and S. Dhara, *Bioresour. Technol.*, 2010, **101**, 3737–3742.
- 21 N. Faraji, W. M. M. Yunus, A. Kharazmi, E. Saion, M. Shahmiri and N. Tamchek, *J. Europ. Opt. Soc. Rap. Public.*, 2012, **7**, 12040–12046.
- 22 Y. Sun, and Y. Xia, *Adv. Mater.*, 2002, **14**, 833–837.
- 23 S. Ghosh, U. Anand and S. Mukherjee, *Analyst*, 2013, **138**, 4270–4274.
- 24 D. Roe, B. Karandikar, N. Bonn-Savage, B. Gibbins and J. Rouillet, *J. Antimicrob. Chemother.*, 2008, **61**, 869–876.
- 25 K. Varaprasad, Y. M. Mohan, K. Vimala and K. M. Raju, *J. Appl. Polym. Sci.*, 2011, **121**, 784–796.
- 26 P. T. S. Kumar, A. K. Manzoor, S. V. Nair, H. Tamura and R. Jayakumar, *Carbohydr. Polym.*, 2010, **80**, 761–767.
- 27 A. Mandal, V. Meda, W. J. Zhang, M. K. Farhan and A. Gnanamani, *Colloids Surf. B.*, 2012, **90**, 191–196.
- 28 A. Mandal, S. Sekar, N. Chandrasekaran, A. Mukherjee and T. P. Sastry, *Proc. Inst. Mech. Eng. Part H*, 2013, **227**, 1224–1236.
- 29 Y. N. Rao, D. Banerjee, A. Datta, S. K. Das, R. Guin and A. Saha, *Radiat. Phys. Chem.*, 2010, **79**, 1240–1246.
- 30 P. Arockianathan, S. Sekar, S. Sankar, B. Kumaran and T. P. Sastry, *Int. J. Biol. Macromol.*, 2012, **50**, 939–946.
- 31 V. Rammath, S. Sekar, S. Sankar and T. P. Sastry, *Int. J. Pharm. Bio Sci.*, 2011, **1**, 577–585.
- 32 M. P. Arockianathan, S. Sekar, S. Sankar, B. Kumaran and T. P. Sastry, *Carbohydr. Polym.*, 2012, **90**, 717–724.
- 33 A. Mandal, S. Sekar, K. M. Seeni Meera, A. Mukherjee, N. Chandrasekaran, T. P. Sastry, *Phys. Chem. Chem. Phys.*, 2014, **16**, 20175–20183.
- 34 W. Zhu, Y. Wu, C. Wang, M. Zhang, and G. Dong, *Nano-Micro Lett.*, 2013, **5**(3), 182–190.
- 35 A. Mandal, T. P. Sastry, *IJIRSET*, 2014, **3**, 12463–12473.
- 36 S. Balaji, R. Kumar, R. Sriprya, U. Rao, A. Mandal, P. Kakkur, P. N. Reddy and P. K. Sehgal, *Polym. Adv. Technol.*, 2012, **23**, 500–507.
- 37 A. J. Kora, S. R. Beedu and A. Jayaraman, *Organic Medicinal Chem. Lett.*, 2012, **2**, 2–10.
- 38 K. J. Sreeram, M. Nidhin and B. U. Nair, *Bull. Mater. Sci.*, 2008, **31**, 937–942.
- 39 J. J. G. Van Soest, H. Tournois, D. de Wit and J. F. G. Vliegthart, *Carbohydr. Res.*, 1995, **279**, 201.
- 40 N. M. Vicentini, N. Dupuy, M. Leitzelman, M. P. Cereda and P. J. A. Sobral, *Spectroscopy Letters*, 2005, **38**, 749.
- 41 Y. Sun, L. Wang, L. Sun, C. Guo, T. Yang, Z. Liu, F. Xu and Z. Li, *J. Chem. Phys.*, 2008, **128**, 074704.
- 42 A. George, and A. Veis, *Biochem.*, 1991, **30**, 2372–2377.
- 43 R. Kumar, R. Sriprya, S. Balaji, M. S. Kumar and P. K. Sehgal, *J. Mol. Struct.*, 2011, **994**, 117.
- 44 S. Krimm and J. Bandekar, *Adv. Prot. Chem.*, 1986, **38**, 181.
- 45 D. Kurouski, T. Postiglione, T. Deckert-Gaudig, V. Deckert and I. K. Lednev, *Analyst*, 2013, **138**, 1665–1673.
- 46 V. B. Bergo, M. Ntefidou, V. D. Trivedi, J. J. Amsden, J. M. Kralj, K. J. Rothschild and J. L. Spudich, *J. Biol. Chem.*, 2006, **281**, 15208–15214.
- 47 A. J. P. Alix, G. Pedanou and M. Berjot, *J. Mol. Struct.*, 1988, **174**, 159.
- 48 S. A. Overman and G. J. Thomas Jr., *Biochem.*, 1998, **37**, 5654.
- 49 J. T. Pelton and L. R. McLean, *Anal. Biochem.*, 2000, **277**, 167.
- 50 R. Schweitzer-Stenner, *Vibrat. Spectrosc.*, 2006, **42**, 98.
- 51 T. Nguyen, T. Happillon, J. Feru, S. Brassart-Passco, J. Angiboust, M. Manfait and O. Piot, *J. Raman Spectrosc.*, 2013, **44**, 1230–1237.
- 52 K. Buckley, P. Matousek, A. W. Parker and A. E. Goodship, *J. Raman Spectrosc.*, 2012, **43**, 1237–1243.
- 53 P. Matejka, B. Vlckova and J. Vohlidal, *J. Phys. Chem.*, 1992, **96**, 1361.
- 54 K. Kalyanasundaram and J. K. Thomas, *J. Phys. Chem.*, 1976, **80**, 1462.
- 55 P. Mukherjee, M. Roy, B. P. Mandal, G. K. Dey, P. K. Mukherjee, J. Ghatak, A. K. Tyagi and S. P. Kale, *Nanotechnol.*, 2008, **19**, 075103–075109.
- 56 Y. Sun, G. Wei, Y. Song, L. Wang, L. Sun, C. Guo, T. Yang and Z. Li, *Nanotechnol.*, 2008, **19**, 115604.
- 57 M. A. M. Khan, S. Kumar, M. Ahamed, S. A. Alrokayan and M. S. AlSalhi, *Nanoscale Res. Lett.*, 2011, **6**, 1–8.
- 58 H. P. Klug and L. E. Alexander, X-ray diffraction procedures for polycrystalline and amorphous materials New York: Wiley; 1954, 491.
- 59 B. Kumar, K. Smita, L. Cumbal, A. Debut and R. N. Pathak, *Bioinorg. Chem. Appl.*, 2014, Article ID 784268, 1–8.

List of Tables**Table 1:** FTIR spectroscopic data of collagen-based scaffolds (C) containing uncapped and different concentrations of sago starch capped AgNPs at 20°C.

Wavenumber (cm ⁻¹)							
C	SG	C-AgNPs	C-SG0.1AgNPs	C-SG0.5AgNPs	C-SG1AgNPs	C-SG5AgNPs	C-SG10AgNPs
3753	3744	3753	3751	3751	3753	3752	3752
3408	3361	3261			3288	3291	3296
-	2924	-	2926	2928	-	-	-
2897	2855	2878			2874	2823	2824
	2151						
1628	1639	1638	1642	1644	1646	1652	1653
1538	1417	1545	1545	1546	1546	1545	1546
1429	1156	1450	1454	1454	1454	1454	1454
1398		1286	1294	1295	1292	1296	1295
1314	1021	1230			1145	1147	1146
1234							
1149		1075	1075	1075	1074	1076	1075
1070					989	996	997
1015	932	950	950	951	953	961	958
872	859	873					
829	764	780	781	783	786	789	789
656	576						
446	527						
	435						

Table 2: FT-Raman spectroscopic data of collagen-based scaffolds containing uncapped and different concentrations of sago starch capped AgNPs at 20°C

Wavenumber (cm ⁻¹)						
C	C-AgNPs	C-SG0.1AgNPs	C-SG0.5AgNPs	C-SG1AgNPs	C-SG5AgNPs	C-SG10AgNPs
2938.7	2938.2	2936.3	2936.6	2938.4	2935.5	2937.1
2880	2879.8					2772.7
2709.9	2709	2755.3	2707.9	2708.7	2707.8	2707.2
	2642.8	2706.1		2552.3	2638.1	2608.5
	1997.7	2204.6		2332.9	2577.7	2547
1661.8	1665.6	2124.9	1669.7	1855.9		2490
	1603.3	2036.2		1670.8		2355
	1450.3	1667.5	1453.2	1451.4	1919	1926
1248.2	1267.5	1455.3		1399.8		1811
	1169.7	1340.	1338.5	1335.5		1762
1034	1089.6	1276	1267.9	1252.2	1655	1673
1004	1062.1	1244.6	1086.8	1084.7	1456.7	1458.6
982.3	999.7	1153.8	983.5	1035.4	1387.8	1386.9
	968.6	1094.6	937.1	1003.9	1333.4	1339.9
920.7		1006.9		977.5	1250	1267.5
	940.1	981.8		940.4	1113.5	1126
859.9	879.5	924.5	860.6	861.8	1079.8	1083
812.1	853.3	856.5		806.8	1000	973.7
	760.1	786.3			934.2	940
	731.9	625.1		679.6	858	857
561.3	552.6	566.3		559.7	774.3	799
		529.8	526.9	529.7	706.4	716
408.1	391.4	442.3	482.8	476.4	556.1	567
			437	446.1	478.8	480
				401	436	430
					357	361
	304.1	314.8, 236.9	318, 294	323.2, 248	320, 230.5	321, 297.2
73.2	74.87	75.6	74.9	74.7	75.2	75.1

Table 3: The $d_{(hkl)}$ values calculated from SAED analysis of collagen based scaffold impregnated with uncapped and different concentrations (0.1-10 μM) of sago starch capped silver nanoparticles.

Sample	Experimental d value (\AA)	JCPDS File No. 04-0783 d value (\AA)	d_{hkl}
C-AgNPs	2.346	2.338	(111)
	2.149	2.039	(200)
	1.698	1.443	(220)
	1.33	1.224	(311)
C-SG0.1AgNPs	2.045	2.338	(111)
	2.342	2.039	(200)
	1.502	1.443	(220)
	1.221	1.224	(311)
C-SG0.5AgNPs	2.361	2.338	(111)
	2.041	2.039	(200)
	1.502	1.443	(220)
	1.216	1.224	(311)
C-SG1AgNPs	2.041	2.039	(111)
	2.352	2.338	(200)
	1.521	1.443	(220)
	1.233	1.224	(311)
C-SG5AgNPs	2.355	2.039	(111)
	2.053	2.338	(200)
	1.531	1.443	(220)
	1.212	1.224	(311)
C-SG10AgNPs	2.401	2.338	(111)
	2.027	2.039	(200)
	1.543	1.443	(220)
	1.237	1.224	(311)

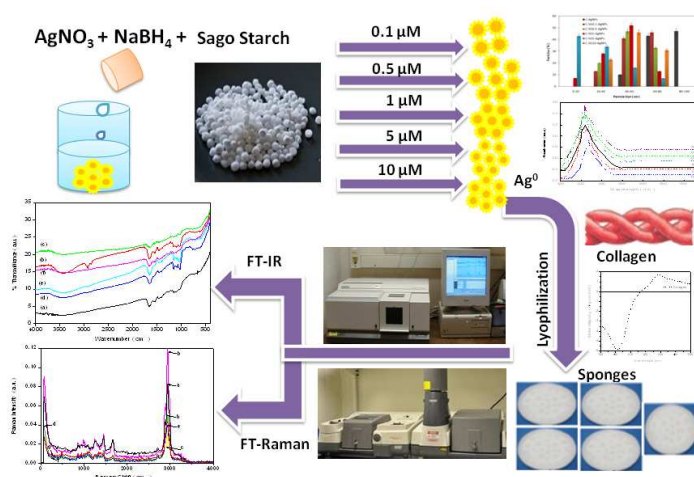
Graphical Abstract

Vibrational spectroscopic investigation on interaction of sago starch capped silver nanoparticles with collagen: A comparative analytical study using FT-IR and FT-Raman techniques

Abhishek Mandal,^{a,b} Santhanam Sekar,^b N. Chandrasekaran,^a
Amitava Mukherjee,^{*a} and Thotapalli P. Sastry^{*b}

^aCentre for Nano-Biotechnology, School of Bio-Sciences and Technology, VIT University, Vellore 632014, India. Tel: +91-416-220 2620; E-mail: amitav@vit.ac.in

^bBio-Products Laboratory, Council of Scientific and Industrial Research (CSIR)-Central Leather Research Institute, Chennai, India. Fax: +91-44-24911589; Tel: +91-44-24420709; E-mail: sastrytp@hotmail.com



Vibrational spectroscopies as analytical tool to investigate interaction of sago starch-capped silver nanoparticles with collagen scaffolds for biomedical applications.